A PHOTOELECTRIC STUDY OF THE ECLIPSING VARIABLE RW TAURI*

GORDON GRANT†
Yerkes and McDonald Observatories
Received August 26, 1958

ABSTRACT

About 300 observations of RW Tauri were obtained on the U, B, V system with the 82- and 13-inch telescopes of the McDonald Observatory. From the depth of the total eclipse of the B star by the K-type subgiant, the magnitudes and colors of the component stars were found. A distance modulus of 8.1 mag. is then derived. A new determination of the variation in period results in an improbably high mass for the unseen campanion. Observations just after the beginning of totality give evidence for a gaseous ring heretofore observed only spectroscopically. The ring extends to 0.1 radius above the surface of the B star with about 0.001 of that star's luminosity. After correction for the intensity of this ring, a photometric solution leads to an upper limit to the limb-darkening coefficient of the B star of 0.3. The small mass function of the K star and its large radius suggest that the star may fill its equipotential surface. If this is the case, the mass ratio is found to be 4.65, which leads to masses of $\mathfrak{M}_B = 2.55\odot$ and $\mathfrak{M}_K = 0.55\odot$. These would make RW Tauri typical of eclipsing systems with a subgiant that is overluminous for its mass. If the equipotential surface were filled, material would be lost to the B star through the inner Lagrangian point and would produce the observed emission ring. From the shape of the equipotential surface the three axes of the elliptical K star are determined. Use of this ellipsoidal model gives a better fit to the observed light-curve, especially near first contact, than does a spherical model.

RW Tauri[1] is a well-known eclipsing system which has the deepest known primary minimum. The B star is totally eclipsed by a K subgiant at intervals of 2.769 days. Total eclipse lasts about 80 minutes. It has been known for many years that the period is variable. Binnendijk (1941) made a photographic study of the system, in which he determined the variation in period and derived a set of elements for the eclipsing pair on the assumption that the limb-darkening coefficient is zero. Joy (1942, 1947) has studied the emission lines, first observed by Wyse (1934), which appear near totality. He postulated a gaseous emission ring which rotates around the B star and is eclipsed with it. Joy also noted a faint visual companion to the binary, separated by 1″ and with $m_V = 12.5$. A spectroscopic study of the eclipsing system was made by Hiltner and Hardie (1949), in which they derived an orbital eccentricity of 0.29.

A photoelectric study in three colors was undertaken to improve our knowledge of the system. In particular, photometric evidence for the presence of the emission ring was sought for, as well as more information on the limb darkening and the character of the secondary star.

I. THE OBSERVATIONS

About 200 observations of RW Tauri on the U, B, V system were obtained on four nights in October, 1955, with a photoelectric photometer attached to the 82-inch reflector at the McDonald Observatory. These were supplemented by about 50 observations in November with the same photometer attached to the 13-inch reflector and an equal number with another photometer on the 82-inch reflector during the primary minimum of November 24, 1955.

* *Contributions from the McDonald Observatory, University of Texas*, No. 293. A portion of a thesis submitted in partial fulfilment of requirements for the Ph.D. degree at the Yerkes Observatory, University of Chicago. Part of the reductions was done while the author was at the Warner and Swasey Observatory of the Case Institute of Technology. This paper was prepared for publication by Helmut Abt after the author's tragic death.

† National Science Foundation Predoctoral Fellow, 1955–1956.

[1] BD+27°623; $\alpha = 3^h57^m8$, $\delta = +27°51'$ (1900); $m_{pg} = 8.0$–12.4; Sp. = B8 Ve, K0 IV.

The photometer for the former observations utilized an unrefrigerated 1P21 photomultiplier. The filter combinations were Corning 9863, Corning 5030 with Schott GG 13, and Corning 3384 for observations in U, B, and V, respectively. A Corning 9863 plus 3384 filter combination was used to test for an infrared leak in the ultraviolet filter; this was found to be negligible for all these observations. A radium spot was used as a standard source for reference throughout each night. The photomultiplier output was amplified by an M.I.T. amplifier whose steps were calibrated in the laboratory. Recording was by a Brown potentiometer whose zero point and rate of paper travel were checked with the observatory Riefler clock. The photometer for the latter observations was kindly lent by Dr. H. L. Johnson.

Comparison stars were b (BD+27°628) and l from the Harvard Chart (Wright 1934); these are close in magnitude and color to RW Tauri at maximum and minimum, respectively. Seven standard stars were chosen from the list of Johnson and Harris (1954) for reduction of these observations to the U, B, V system. Table 1 gives the magnitudes and colors of the standard and comparison stars as determined in this study.

TABLE 1

PHOTOMETRY OF STANDARD AND COMPARISON STARS

Star	V	$B-V$	$U-B$	Sp.
υ Ori. ..	4 63	−0.26	−1.07	B0 V
η Aur ..	3.17	−0.18	−0.67	B3 V
HR 1046 .	5 08	+0 05	+0.03	A1 V
π^3 Ori. .	3.19	+0.45	−0.01	F8 V
ϵ Tau .	3.54	+1.02	+0.88	K0 III
β Cnc . ..	3.53	+1.478	+1.77	K4 III
χ Peg.	4.80	+1.58	+1.92	M2 III
b: BD +27°628.....	7.912	+0 094	+0.020	A3
l	11 058	+1.093	+0 812	K1 III–V

The observing procedure for the non-variable stars and for RW Tauri outside eclipse was to make symmetric observations in the three magnitudes. During the eclipse, however, the rapidity of the light-change made symmetric observations unfeasible, so that individual deflections of 20–30 seconds were recorded. An individual set was of the form B–V–U–B–V–U–B, so that the $B-V$ and $U-B$ colors could be found by interpolation. Sky readings were taken before and after each set. As the $B-V$ color of RW Tauri changes by nearly a magnitude during eclipse, corrections depending on color must be accurately made. Reduction procedures outlined by Johnson and Morgan (1951) and Sharpless (1952) were adopted. The extinction coefficients for each night were determined from the comparison stars. Magnitudes in the natural system were reduced to outside the atmosphere and converted to the U, B, V system through the transfer equations determined from the standard stars. These magnitudes are listed in Table 2. The phases were computed from Binnendijk's (1941) short-term ephemeris with a correction in epoch (Table 4) determined from the present observations.

II. MAGNITUDES AND COLORS

The magnitudes of RW Tauri outside eclipse may be derived from the measures during phases 0.1–0.4 and 0.6–0.9. The U, B, V magnitudes during these phases are essentially constant (Table 2); hence no rectification is required. The weighted means for these magnitudes are found in line 1 of Table 3. The magnitudes during primary minimum are found by averaging the values from phases between 0.995 and 0.010 and are

TABLE 2

PHOTOELECTRIC OBSERVATIONS OF RW TAURI
Ultraviolet Magnitudes

Helioc. JD 2435000+	Helioc. Phase	U	Helioc. JD 2435000+	Helioc. Phase	U	Helioc. JD 2435000+	Helioc. Phase	U
408.8215	0.91505	7.879	411.7075	0.95736	8.354	411.8329	0.00263	13.179
408.8250	0.91631	7.901	411.7086	0.95773	8.366	411.8346	0.00326	13.128
408.8285	0.91756	7.876	411.7096	0.95811	8.381	411.8445	0.00682	13.151
408.8382	0.92107	7.872	411.7115	0.95877	8.396	411.8465	0.00754	13.173
408.8430	0.92283	7.881	411.7124	0.95912	8.409	411.8482	0.00814	13.187
408.8465	0.92408	7.889	411.7136	0.95954	8.426	411.8501	0.00885	13.129
408.8514	0.92584	7.889	411.7193	0.96162	8.504	411.8588	0.01199	11.888
408.8604	0.92910	7.887	411.7204	0.96200	8.526	411.8611	0.01281	11.564
408.8645	0.93060	7.896	411.7214	0.96235	8.538	411.8626	0.01336	11.348
408.8687	0.93211	7.913	411.7237	0.96318	8.572	411.8642	0.01391	11.146
408.8729	0.93336	7.922	411.7247	0.96355	8.592	411.8660	0.01456	10.966
408.8819	0.93687	7.961	411.7258	0.96393	8.618	411.8700	0.01602	10.542
408.8889	0.93938	7.990	411.7353	0.96739	8.779	411.8714	0.01655	10.414
408.8916	0.94038	8.008	411.7364	0.96776	8.807	411.8718	0.01667	10.360
408.8958	0.94189	8.014	411.7374	0.96811	8.816	411.8743	0.01757	10.201
408.9042	0.94490	8.064	411.7405	0.96925	8.883	411.8766	0.01841	10.067
408.9076	0.94615	8.096	411.7415	0.96960	8.902	411.8843	0.02119	9.682
408.9111	0.94741	8.157	411.7426	0.97000	8.930	411.8858	0.02174	9.602
408.9187	0.95017	8.179	411.7481	0.97201	9.061	411.8870	0.02217	9.564
408.9236	0.95192	8.218	411.7492	0.97241	9.090	411.8899	0.02319	9.447
408.9271	0.95318	8.236	411.7502	0.97276	9.115	411.8918	0.02392	9.384
409.717	0.2384	7.800	411.7522	0.97346	9.177	411.8944	0.02485	9.308
409.718	0.2389	7.795	411.7533	0.97386	9.203	411.8956	0.02528	9.267
409.719	0.2394	7.798	411.7544	0.97426	9.234	411.8968	0.02570	9.254
409.725	0.2414	7.791	411.7605	0.97647	9.426	411.9070	0.02939	8.962
409.727	0.2421	7.799	411.7615	0.97682	9.459	411.9089	0.03006	8.916
409.728	0.2426	7.790	411.7629	0.97732	9.509	411.9109	0.03080	8.871
409.780	0.2614	7.777	411.7658	0.97813	9.612	411.9126	0.03142	8.831
409.786	0.2634	7.783	411.7669	0.97853	9.674	411.9155	0.03242	8.770
409.788	0.2642	7.788	411.7683	0.97903	9.717	411.9169	0.03297	8.743
409.790	0.2647	7.786	411.7797	0.98344	10.378	411.9181	0.03343	8.717
409.799	0.2680	7.786	411.7826	0.98447	10.589	411.9198	0.03401	8.691
409.800	0.2685	7.786	411.7840	0.98497	10.716	411.9281	0.03699	8.553
409.802	0.2692	7.791	411.7855	0.98552	10.872	411.9295	0.03754	8.527
409.804	0.2697	7.788	411.7869	0.98602	11.005	411.9308	0.03799	8.515
409.806	0.2705	7.783	411.7883	0.98652	11.196	411.9323	0.03852	8.510
409.808	0.2712	7.786	411.7898	0.98706	11.357	411.9337	0.03902	8.479
410.776	0.6208	7.767	411.7965	0.98948	12.615	411.9352	0.03957	8.458
410.779	0.6218	7.766	411.7992	0.99047	12.879	411.9365	0.04003	8.445
410.782	0.6230	7.765	411.8006	0.99094	12.986	411.9380	0.04058	8.420
411.6774	0.94644	8.084	411.8024	0.99159	13.021	411.9395	0.04113	8.400
411.6779	0.94663	8.093	411.8041	0.99219	13.073			
411.6796	0.94723	8.099	411.8059	0.99287	13.060			
411.6807	0.94765	8.110	411.8137	0.99568	13.108			
411.6950	0.95285	8.227	411.8142	0.99585	13.108			
411.6969	0.95352	8.241	411.8161	0.99654	13.140			
411.6981	0.95395	8.257	411.8185	0.99744	13.192			
411.6993	0.95437	8.269	411.8198	0.99789	13.194			
411.7005	0.95480	8.276	411.8288	0.00112	13.130			
411.7018	0.95525	8.290	411.8314	0.00210	13.180			

TABLE 2 (Continued)—Blue Magnitudes

Helioc. JD 2435000+	Helioc. Phase	B	Helioc. JD 2435000+	Helioc. Phase	B	Helioc. JD 2435000+	Helioc. Phase	B
408.8215	0.91505	8.075	411.6768	0.94625	8.260	411.7903	0.98723	11.456
408.8250	0.91631	8.083	411.6784	0.94683	8.276	411.7955	0.98911	12.184
408.8285	0.91756	8.069	411.6789	0.94698	8.269	411.7980	0.99001	12.391
408.8382	0.92107	8.064	411.6800	0.94740	8.282	411.7997	0.99062	12.472
408.8430	0.92283	8.071	411.6812	0.94780	8.286	411.8012	0.99117	12.456
408.8465	0.92408	8.070	411.6944	0.95262	8.414	411.8029	0.99177	12.459
408.8514	0.92584	8.069	411.6962	0.95325	8.418	411.8045	0.99237	12.480
408.8604	0.92910	8.071	411.6974	0.95370	8.432	411.8063	0.99305	12.485
408.8632	0.93010	8.079	411.6986	0.95412	8.453	411.8127	0.99533	12.503
408.8660	0.93110	8.085	411.6999	0.95457	8.463	411.8146	0.99600	12.541
408.8666	0.93136	8.086	411.7011	0.95500	8.471	411.8150	0.99615	12.544
408.8701	0.93261	8.092	411.7022	0.95541	8.489	411.8165	0.99669	12.546
408.8715	0.93311	8.103	411.7068	0.95711	8.548	411.8189	0.99759	12.513
408.8743	0.93411	8.108	411.7079	0.95748	8.551	411.8204	0.99811	12.494
408.8805	0.93637	8.134	411.7090	0.95788	8.564	411.8279	0.00082	12.487
408.8833	0.93738	8.151	411.7108	0.95851	8.575	411.8294	0.00135	12.504
408.8875	0.93888	8.174	411.7119	0.95892	8.580	411.8305	0.00177	12.524
408.8896	0.93963	8.176	411.7129	0.95929	8.595	411.8320	0.00233	12.504
408.8903	0.93988	8.180	411.7140	0.95967	8.620	411.8334	0.00283	12.524
408.8930	0.94089	8.190	411.7187	0.96139	8.682	411.8351	0.00343	12.527
408.8951	0.94164	8.191	411.7198	0.96178	8.704	411.8433	0.00639	12.506
408.8972	0.94239	8.197	411.7207	0.96213	8.727	411.8455	0.00719	12.542
408.9028	0.94440	8.228	411.7231	0.96298	8.748	411.8473	0.00784	12.523
408.9055	0.94540	8.248	411.7241	0.96333	8.772	411.8487	0.00833	12.507
408.9069	0.94590	8.258	411.7251	0.96370	8.795	411.8506	0.00900	12.528
408.9090	0.94666	8.289	411.7261	0.96405	8.817	411.8573	0.01145	11.970
408.9097	0.94691	8.302	411.7346	0.96714	8.961	411.8595	0.01224	11.666
408.9125	0.94791	8.344	411.7357	0.96751	8.986	411.8617	0.01301	11.425
408.9174	0.94966	8.338	411.7367	0.96789	9.000	411.8631	0.01354	11.258
408.9201	0.95067	8.372	411.7379	0.96832	9.019	411.8648	0.01414	11.116
408.9222	0.95142	8.381	411.7400	0.96905	9.058	411.8691	0.01570	10.687
408.9250	0.95242	8.416	411.7409	0.96940	9.083	411.8706	0.01625	10.571
408.9257	0.95267	8.405	411.7420	0.96977	9.097	411.8734	0.01725	10.396
408.9285	0.95368	8.441	411.7430	0.97015	9.119	411.8752	0.01816	10.247
409.715	0.2379	8.037	411.7474	0.97176	9.221	411.8772	0.01863	10.174
409.717	0.2386	8.038	411.7486	0.97218	9.252	411.8834	0.02087	9.874
409.719	0.2391	8.036	411.7497	0.97256	9.276	411.8848	0.02137	9.819
409.724	0.2411	8.028	411.7515	0.97321	9.322	411.8862	0.02189	9.753
409.726	0.2416	8.038	411.7526	0.97361	9.361	411.8887	0.02277	9.663
409.727	0.2421	8.035	411.7538	0.97403	9.386	411.8903	0.02334	9.612
409.780	0.2612	8.024	411.7548	0.97441	9.427	411.8907	0.02349	9.602
409.785	0.2629	8.036	411.7597	0.97619	9.580	411.8922	0.02404	9.532
409.787	0.2637	8.039	411.7608	0.97659	9.624	411.8938	0.02463	9.507
409.788	0.2642	8.042	411.7619	0.97699	9.657	411.8949	0.02503	9.463
409.790	0.2649	8.044	411.7651	0.97813	9.761	411.8961	0.02545	9.434
409.797	0.2675	8.032	411.7662	0.97853	9.815	411.8973	0.02588	9.400
409.799	0.2680	8.038	411.7674	0.97895	9.847	411.9061	0.02906	9.180
409.801	0.2687	8.038	411.7687	0.97945	9.922	411.9075	0.02956	9.153
409.803	0.2695	8.039	411.7791	0.98316	10.489	411.9079	0.02971	9.145
409.805	0.2702	8.030	411.7820	0.98425	10.677	411.9094	0.03025	9.103
409.806	0.2707	8.034	411.7832	0.98467	10.767			
409.809	0.2717	8.031	411.7846	0.98520	10.889			
410.776	0.6208	8.027	411.7861	0.98572	11.027			
410.779	0.6218	8.028	411.7875	0.98622	11.153			
410.782	0.6230	8.028	411.7889	0.98672	11.284			

TABLE 2 (Concluded)—Visual Magnitudes

Helioc. JD 2435000+	Helioc. Phase	V	Helioc. JD 2435000+	Helioc. Phase	V	Helioc. JD 2435000+	Helioc. Phase	V
408.8215	0.91505	8.028	410.776	0.6208	7.967	411.7959	0.98926	11.339
408.8250	0.91631	8.040	410.779	0.6218	7.965	411.7984	0.99016	11.454
408.8285	0.91756	8.023	410.782	0.6230	7.959	411.8001	0.99079	11.456
408.8382	0.92107	8.026	411.6771	0.94634	8.216	411.8019	0.99142	11.443
408.8430	0.92283	8.026	411.6782	0.94665	8.229	411.8033	0.99192	11.448
408.8465	0.92408	8.030	411.6792	0.94710	8.231	411.8052	0.99264	11.451
408.8514	0.92584	8.027	411.6804	0.94753	8.243	411.8133	0.99553	11.462
408.8604	0.92910	8.026	411.6947	0.95272	8.362	411.8156	0.99636	11.461
408.8639	0.93035	8.041	411.6966	0.95340	8.377	411.8181	0.99704	11.475
408.8653	0.93085	8.041	411.6977	0.95380	8.385	411.8193	0.99749	11.463
408.8673	0.93161	8.046	411.6990	0.95427	8.399	411.8282	0.00092	11.458
408.8694	0.93236	8.047	411.7002	0.95470	8.405	411.8309	0.00190	11.487
408.8722	0.93336	8.050	411.7014	0.95512	8.414	411.8324	0.00246	11.476
408.8736	0.93386	8.061	411.7072	0.95723	8.485	411.8339	0.00298	11.476
408.8812	0.93662	8.096	411.7082	0.95761	8.494	411.8437	0.00654	11.465
408.8826	0.93712	8.101	411.7094	0.95801	8.511	411.8461	0.00739	11.472
408.8882	0.93913	8.126	411.7111	0.95864	8.526	411.8477	0.00797	11.473
408.8896	0.93963	8.127	411.7122	0.95902	8.529	411.8497	0.00867	11.490
408.8910	0.94013	8.138	411.7133	0.95942	8.551	411.8584	0.01184	11.158
408.8923	0.94064	8.141	411.7191	0.96152	8.626	411.8601	0.01244	11.026
408.8951	0.94164	8.146	411.7200	0.96188	8.649	411.8622	0.01319	10.907
408.8965	0.94214	8.150	411.7210	0.96223	8.658	411.8637	0.01374	10.758
408.9035	0.94465	8.190	411.7234	0.96308	8.683	411.8654	0.01434	10.646
408.9048	0.94515	8.197	411.7244	0.96343	8.704	411.8695	0.01585	10.347
408.9069	0.94590	8.217	411.7254	0.96380	8.723	411.8710	0.01640	10.224
408.9083	0.94640	8.232	411.7350	0.96726	8.875	411.8737	0.01737	10.110
408.9104	0.94716	8.258	411.7360	0.96764	8.896	411.8762	0.01826	10.002
408.9118	0.94766	8.277	411.7370	0.96799	8.908	411.8838	0.02102	9.683
408.9180	0.94992	8.296	411.7402	0.96915	8.964	411.8851	0.02149	9.648
408.9194	0.95042	8.312	411.7412	0.96950	8.984	411.8866	0.02202	9.583
408.9129	0.95167	8.340	411.7423	0.96990	9.004	411.8891	0.02292	9.504
408.9143	0.95217	8.346	411.7478	0.97191	9.115	411.8915	0.02377	9.423
408.9164	0.95292	8.362	411.7489	0.97228	9.146	411.8941	0.02473	9.350
408.9278	0.95343	8.368	411.7499	0.97266	9.164	411.8952	0.02513	9.321
409.716	0.2381	7.977	411.7518	0.97331	9.213	411.8964	0.02558	9.292
409.718	0.2389	7.977	411.7529	0.97373	9.244	411.9066	0.02924	9.057
409.719	0.2394	7.975	411.7541	0.97413	9.273	411.9083	0.02986	9.012
409.725	0.2414	7.972	411.7600	0.97629	9.453	411.9100	0.03047	8.988
409.726	0.2419	7.977	411.7612	0.97672	9.491	411.9113	0.03095	8.954
409.728	0.2424	7.971	411.7624	0.97714	9.510	411.9122	0.03127	8.938
409.780	0.2614	7.968	411.7654	0.97825	9.608	411.9150	0.03225	8.890
409.785	0.2632	7.966	411.7666	0.97865	9.653	411.9164	0.03280	8.861
409.787	0.2639	7.971	411.7678	0.97910	9.688	411.9178	0.03327	8.834
409.789	0.2644	7.967	411.7794	0.98331	10.211	411.9190	0.03373	8.818
409.798	0.2677	7.966	411.7823	0.98435	10.346	411.9275	0.03679	8.689
409.799	0.2682	7.966	411.7836	0.98482	10.429	411.9290	0.03732	8.673
409.801	0.2690	7.980	411.7851	0.98535	10.517	411.9303	0.03782	8.657
409.803	0.2695	7.971	411.7865	0.98587	10.613	411.9317	0.03832	8.634
409.805	0.2702	7.964	411.7880	0.98640	10.722	411.9332	0.03884	8.628
409.807	0.2710	7.965	411.7894	0.98690	10.813	411.9348	0.03942	8.588
						411.9360	0.03988	8.566
						411.9375	0.04040	8.544
						411.9390	0.04095	8.535

given in line 2. The depth of the primary eclipse follows (line 3) and from this the magnitudes of the B star itself may be determined (line 4). Using Johnson and Morgan's (1953) parameter Q, which is independent of interstellar reddening, the intrinsic colors of the B star are found, and these correspond to spectral class B8. The color excesses and total absorption may then be found by means of Hiltner and Johnson's (1956) equations of the mean reddening line and the ratio of total to selective absorption. These corrections, listed in line 5, are applied in line 6 to give the magnitudes and colors for the B star corrected for interstellar absorption. This star will be shown to be on the main sequence, but its age and hence its evolution away from the zero-age main sequence are not known. A value of M_V(B8 V) = −0.5 is adopted from Keenan and Morgan (1951), leading to a distance modulus of 8.1 mag. or a distance of 420 parsecs.

The combined visual magnitude of the secondary component, K, and the visual companion, C, is observed to be 11.47. With Joy's visual magnitude for C of 12.5, the apparent magnitude of K (uncorrected for interstellar absorption) is about 12.0, so that the visual difference V(K + C) − V(K) = −0.5 mag. The combined magni-

TABLE 3

PHOTOMETRIC DATA FOR RW TAURI

	V	$B-V$	B	$U-B$	U
1. Outside eclipse	7 975	+0 059	8 034	−0 256	7.778
2. Primary minimum	11 472	+1 047	12 519	+ .635	13 154
3. Depth of eclipse	3.497	+0 988	4 485	+ .891	5.376
4 Magnitudes and colors of B star	8 019	+0 033	8.052	− .266	7 786
5. A_V, E_{B-V}, E_{U-B}	0.420	+0 140	...	+ .102	...
6. Corrected mag. and colors of B	7 60	−0 11	7 49	− .37	7.12
7. Same for K+C	11 05	+0 91	11.96	+ .53	12.49
8. Standard colors for K0 III	.....	+1.01	.....	+ .86	.....
9. Standard colors for K0 V.	.....	+0.82	.....	+0.48	.....
10. L(B)	0.9601		0 9839		0.9929
11. L(K)	.0243		.0098		0043
12. L(C)	0.0156		0.0063		0.0028

tudes of K and C, corrected for absorption as above, are given in line 7. With this value and the magnitude difference, the corrected visual magnitude of the K star is 11.5. This distance modulus then gives M_V(K0 IV) = +3.4, which happens to be equal to Keenan and Morgan's (1951) value for a K0 IV star. If C is a physical companion, M_V(C) = +3.9. The average colors for K0 III and K0 V stars are given in lines 8 and 9 (Johnson and Morgan 1953). It is seen that the K + C colors are intermediate. Since the K star is known to be of type K0 IV from spectroscopic and photometric data, the color of the visual companion cannot be very different. If these colors are equal, the luminosities, L(K) and L(C), can be found along with L(B) (lines 10–12), where L(B) + L(K) + L(C) = 1.000.

III. VARIATION OF PERIOD

Determinations of the times of minima from the present observations were made for October 31, November 25, and December 5, 1955, when both branches of the light-curve were observed. The times of minimum on the first two dates were determined in the three magnitudes by Hertzsprung's (1928) method, and a mean value for each date was obtained. For December 5, which had fewer observations, a graphical method was used. These times of minima are given in Table 4 along with other recent results. The (O − C) values with respect to Binnendijk's short-term ephemeris show that the

period is definitely lengthening again, as predicted in Dugan and Wright's (1938) study. They made the assumption that the variation is due to a change in light-time from revolving around a third body.

It will require observations over the next few years to establish the period and amplitude of the long-term variation accurately, but an estimate may be made from the present material. Figure 1 shows the residuals of the Harvard photographic observations (Dugan and Wright 1938), Binnendijk's (1941) visual and photographic normals, and the recent data (Table 4). A curve through the residuals will again cross the zero axis on the ascending branch, but its subsequent shape is still not well defined. The mean period as defined by Figure 1 is given by the ephemeris:

$$\text{Min.} = 2417198.410 + 2.7688463E\ . \qquad (1)$$

TABLE 4

TIMES OF PRIMARY MINIMA OF RW TAURI

Observer	Minimum JD	Cycle E	(O−C) Binn.	Reference
Lange.....	2429871 409	887	−0^{d}001	*Astr. Circ. U.S.S.R.*, **13**, 6, 1943
	30760 206	1208	+ 006	
Szafraniec.....	32850 665	1963	+ 009	*Acta Astr.*, Ser. c, **4**, 113, 1950
Vasulbeva...	32881 123	1974	+ 010	*Astr. Circ. U.S.S.R.*, **103–104**, 2, 1950
Piotrowski . .	32889 430	1977	+ 011	*Acta Astr.*, Ser. c, **4**, 129, 1951
Lenouvel....	33620 3979	2241	+ 0111	*J. Obs.*, **34**, 13, 1951
	34423 3596	2531	+ 0161	*Ibid.*, **37**, 137, 1954
Szafraniec.....	34661 477	2617	+ 015	*Acta Astr.*, Ser. c, **5**, 189, 1955.
	35010 352	2743	+ 019	*Ibid.*, p. 193
	35071 263	2765	+ 017	*Ibid.*, p. 193
Grant.... .	35411 8256	2888	+ 0148	Present study
	35436 7452	2897	+ 0150	
	35447 8208	2901	+0 0153	

The curve leads to the provisional value of $P' = 8000P$, semiamplitude = 0^{d}064, $e = 0.25$, and $\omega = 45°$. The light-time correction from the semiamplitude gives $a \sin i = 11$ A.U.; the period would be 61 years. The resulting mass function is

$$\left(\frac{\mathfrak{M}_D \sin i}{\mathfrak{M}_B + \mathfrak{M}_K + \mathfrak{M}_D}\right)^3 (\mathfrak{M}_B + \mathfrak{M}_K + \mathfrak{M}_D) = 0.36\odot\ , \qquad (2)$$

which is surprisingly large; D is the hypothetical fourth body responsible for the change. If $\mathfrak{M}_B + \mathfrak{M}_K = 3.1\ \odot$ (Sec. V) for the mass of the eclipsing pair, the mass of D comes out to be 3.0 $\odot$. If $\mathfrak{M}_B = 2.55\ \odot$ and if $L \propto \mathfrak{M}^4$, $L_D/L_B = 2$, which is clearly incompatible with the observed eclipse. It seems difficult to account for any significant amount of light coming from D. As the preceding section seems to account satisfactorily for the observed magnitudes and colors of the component stars, any large contribution of light by a fourth body seems photometrically unacceptable. Perhaps D is one or several white dwarfs if the variation in period is to be explained by a change in light-time.

IV. THE LIGHT-CURVE AND ITS FORMAL SOLUTION

The observations of October 31 show systematic deviations (0.02 mag. in V, 0.05 in B, and 0.10 in U) near the beginning of totality, as compared with the remainder of the minimum (Fig. 2). The November 24 eclipse observations (not plotted) show

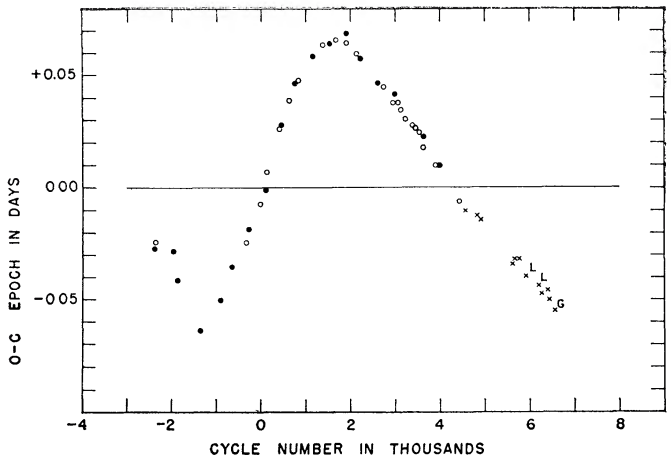

FIG. 1.—Time residuals of primary minima as computed from the long-term ephemeris. The filled circles are determinations by Dugan and Wright, and the open circles by Binnendijk. The recent photoelectric data are designated by *L* (Lenouvel) and *G* (Grant) above and to the right of the symbol.

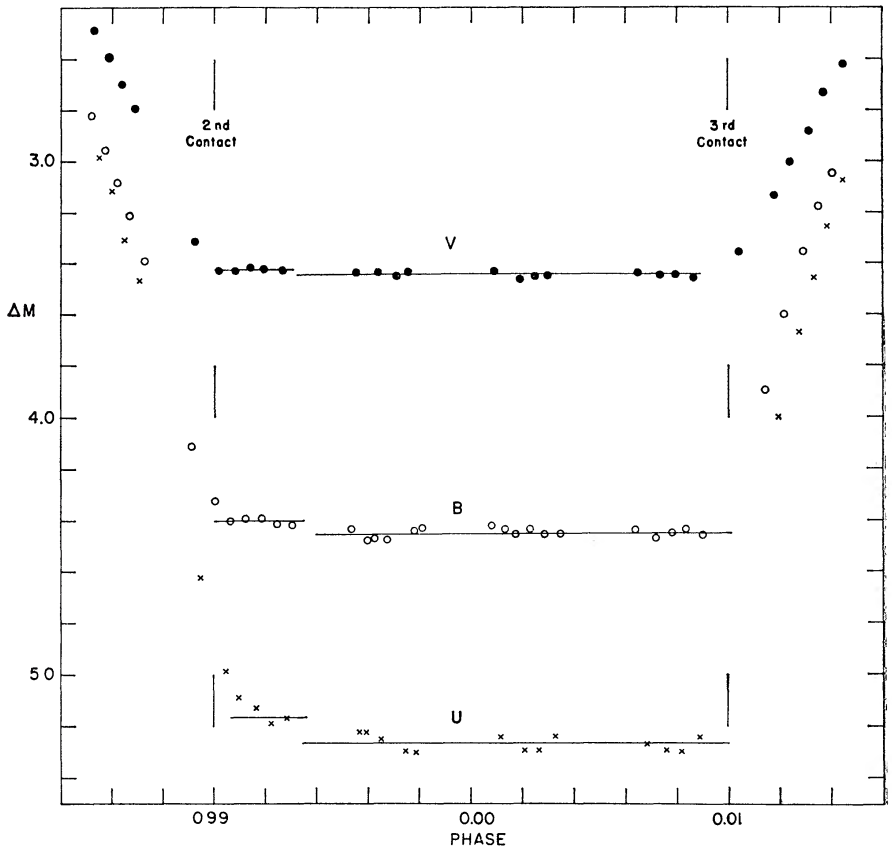

FIG. 2.—The light-curve near primary minimum. Individual observations, expressed in units of the depth of eclipse in magnitudes, are plotted against phase. The residual light present after second contact is evident.

a similar effect, so these deviations are felt to be real. This residual light is probably due to the gaseous ring observed spectroscopically by Joy (1942). The gaseous ring extends beyond the surface of the B star and thus is still partially visible after the beginning of totality ($0.990P$). This ring becomes eclipsed soon after $0.993P$. Since the B star travels 0.1 of its radius in $0.0033P$, the ring must extend to about 0.1 R_B above the B star. As the intensity is relatively constant from 0.990 to $0.993P$, a single condensation would fit the observations as well. There is no photometric evidence for a ring appearing just before egress; this is consistent with Joy's (1947) spectroscopic observations.

The color of the ring may be found by converting the residual light observed in the three spectral regions to intensity units. Referring the data to unit light at 11.50 mag., the ring contributes 0.024 to ultraviolet light, 0.017 to the blue, and 0.020 to the visual. Thus its color is similar to the B star. The total intensity, however, is less than 0.001 of the B star. In the solution of the light-curve the observations just outside totality are corrected by subtracting the contribution from the ring, taking the intensity of the ring during totality as the contributed light.

The observations made with the 82-inch reflector on October 28 and 31 entirely covered the partial phases of the eclipse, the minimum, and the parts of the adjacent maxima. The latter differ slightly from the maximum brightness adopted in Section III. On plotting the magnitudes against cos θ or cos 2θ, the measures outside eclipse show no clear ellipticity or reflection effect. In the case of the U observations, however, there is a departure from constancy just outside the eclipse proper, requiring a correction of 0.005 mag. at totality. At the other wave lengths no corrections are necessary, and the maximum light just outside eclipse is adopted. A more extensive series of observations outside eclipse would be necessary to determine whether any other rectification is necessary.

The observations mentioned above form a homogeneous set, and the analysis of the light-curve is based on them alone. A different photometer was used on November 24, and only the deepest portion of the minimum was observed. Only small segments of the partial phases were observed on other nights, and little weight would be added by including them in the solution. Because of the shallowness of the secondary minimum (about 0.004 mag. in U), this minimum was not used in the solution except as a check.

As the magnitude during totality and that outside eclipse are known with sufficient accuracy, no correction to these quantities need be included in the solution. The solution then depends only on the shape of the light-curve during the partial phases. This procedure has the advantage that it does not depend on the distribution of light between the eclipsing star and a third body. This latter factor enters, however, in the determination of the surface brightnesses.

The three magnitudes outside eclipse are subtracted from all the magnitudes during eclipse and these differences are converted to light units. The values of l_U, l_B, and l_V outside eclipse are each taken as 1.000. The l-values are plotted against $\sin^2\theta$, found from the phases, where $\theta = 2\pi \times$ phase. Such a plot has less curvature than if the magnitudes were plotted directly, thus facilitating the formation of normals. Normals were formed by averaging the (l, $\sin^2\theta$) values within the group. Fewer observations per normal were taken near minimum. Table 5 lists for each spectral region the number of observations, n; $\sin^2\theta$; l; the square root of the weight, w, of the normal; and the O − C residuals from the final light-curve. The weights used will be discussed below. For $l < 0.50$, the intensities are given to four places, as the errors in light-units are smaller. The $\sin^2\theta$ values are carried to a corresponding number of significant figures.

The fractional depth of the eclipse, α, is determined for all normals, where

$$\alpha = \frac{1 - l}{1 - l_0} \tag{3}$$

TABLE 5

ULTRAVIOLET NORMAL POINTS

n	$\sin^2\theta$	l	$\sqrt{w}$	(O−C) $\sin^2\theta$
2.....	0.00500	0.0190	36	−0.00013
2.....	.00652	.0374	36	+ .00001
2.....	.00708	.0444	34	+ .00007
2.....	.00764	.0532	32	+ .00004
2.....	.00828	.0614	29	+ .00012
2.....	.00918	.0786	25	− .00015
2.....	.01042	.0918	22	+ .00018
2.....	.01086	.1018	20	− .00007
2.....	.01270	.1267	18	+ .00000
3.....	.01770	.1902	18	+ .00019
4.....	.01918	.2124	19	− .00015
4.....	.02155	.2422	17	− .00028
4.....	.02524	.2814	15	− .00009
5.....	.02872	.3195	14	− .00035
4.....	.03502	.3840	11	− .00057
5.....	.03846	.4156	9	− .00066
5.....	.04261	.4564	8	− .00132
5.....	.05240	.533	6	− .00148
5.....	.0562	.559	5	− .0014
5.....	.0616	.599	4.5	− .0019
6.....	.0670	.633	4.5	− .0020
4.....	.0792	.701	3.5	− .0018
5.....	.0870	.736	3.0	− .0008
5.....	.1076	.829	2.0	− .0015
4.....	.1287	.886	1.5	+ .0034
4.....	0.1660	0.965	1.0	+0.0093
	Blue Normal Points			
2.....	0.00492	0.0251	36	+0.00006
2.....	.00617	.0404	39	+ .00000
2.....	.00680	.0489	35	+ .00000
2.....	.00734	.0556	33	+ .00020
2.....	.00795	.0631	31	+ .00015
2.....	.00890	.0790	26	− .00002
3.....	.00990	.0935	30	− .00003
2.....	.01143	.1126	23	+ .00014
2.....	.01330	.1395	18	− .00019
3.....	.01702	.1889	18	− .00004
4.....	.01838	.2060	19	− .00007
5.....	.02111	.2376	18	+ .00001
4.....	.02328	.2634	17	− .00008
4.....	.02590	.2909	15	+ .00002
5.....	.02933	.3268	14	+ .00001
4.....	.03406	.3705	11	+ .00026
5.....	.03658	.3955	11	+ .00007
5.....	.03980	.4246	9	+ .00002
5.....	.04311	.4553	8	− .00029
6.....	0.0520	0.524	7	−0.0002

TABLE 5—*Continued*

n	$\sin^2\theta$	l	$\sqrt{w}$	$(O-C)\sin^2\theta$
	Blue Normal Points—*Continued*			
6.....	0.0565	0.556	6	+0.0000
6.....	.0624	.598	5	− .0004
6.....	.0678	.632	4.5	− .0005
7.....	.0804	.704	4.0	− .0005
6.....	.0898	.747	3.5	+ .0003
5.....	.1061	.822	2.5	− .0004
5.....	.1119	.843	2.0	+ .0000
5.....	.1317	.899	1.5	+ 0030
4.....	.1502	.957	1.0	+ 0073
5.....	0.1733	0.984	1.0	+0.0052
	Visual Normal Points			
2.....	0.00582	0.0595	38	+0.00018
2.....	.00681	.0736	35	+ .00015
2.....	.00736	.0822	33	+ .00008
2.....	.00800	.0910	31	+ .00009
2.....	.00876	.1052	27	− .00013
2.....	.00976	.1180	25	− .00004
2.....	.01076	.1330	23	− .00010
2.....	.01248	.1545	20	+ .00005
4.....	.01762	.2206	20	+ .00004
4.....	.01966	.2459	18	− .00005
4.....	.02234	.2744	17	+ .00012
4.....	.02587	.3128	15	+ .00005
4.....	.02948	.3526	13	− .00030
5.....	.03520	.4032	11	− .00002
5.....	.03859	.4351	9	− .00032
5.....	.04234	.4658	8	− .00031
5.....	.0524	.541	7	− .0002
5.....	.0562	.566	6	− .0001
5.....	.0613	.604	5	− .0008
6.....	.0673	.639	4.5	− .0005
6.....	.0808	.715	4.0	− .0010
6.....	.0896	.752	3.5	+ .0002
6.....	.1074	.826	2.5	+ .0004
5.....	.1192	.869	1.5	+ .0002
6.....	.1405	.917	1.0	+ .0054
6.....	0.1715	0.981	1.0	+0.0055

and l_0 is the value of l during totality. In the preliminary solution, a is plotted against $\sin^2\theta$, and a smooth curve is drawn; thus $\sin^2\theta$ may be found for any value of a. The quantity ψ may be defined (Russell and Merrill 1952) as

$$\psi(x, k, a_i) = \frac{\sin^2\theta\,(a = a_i) - \sin^2\theta\,(a = 0.6)}{\sin^2\theta\,(a = 0.6) - \sin^2\theta\,(a = 0.9)}. \quad (4)$$

Thus ψ is a function of the limb darkening, x, the ratio of radii, k, and a_i. With an assumed value of x, a value of k is found for each a_i from the ψ tables (Merrill 1950). If general agreement between the various k's is found, a mean value may be safely adopted. The inclination of the orbit may be determined from

$$\cot^2 i = \frac{B}{\phi_2(k, x)} - A \tag{5}$$

(Russell and Merrill 1952), where $B = \sin^2\theta\ (a = 0.6) - \sin^2\theta\ (a = 0.9)$ and $A = \sin^2\theta\ (a = 0.6)$; ϕ_2 is also tabulated by Merrill (1950). Clearly, $\phi_2(x, k) \leq B/A$, in order that i may be real. The quantity ϕ_2 increases with increasing k and also with increasing x. In the case of the observations in blue light under consideration, $B/A = 0.6995$. If $x = 0$, then $k \leq 0.738$, while if $x = 0.4$, then $k \leq 0.753$. Eighty per cent of the weight of the normals is in the interval $0.900 < a < 0.992$. In this interval the ψ tables give $k = 0.71$ if $x = 0$; this leads to $i = 87.85°$, r_K (the radius of the K star) $= 0.2494$, and r_B (the radius of the B star) $= 0.1769$. The extreme limit $i = 90°$ is reached for $x = 0.3$; then $k = 0.749$, $r_K = 0.2469$, and $r_B = 0.1852$. Therefore, we come to the conclusion that, for spherical stars, no value of the limb-darkening coefficient larger than 0.3 is compatible with the observations. Similar results are found for the U and V magnitudes.

TABLE 6

COMPARISON OF EXTREME MODELS AND OBSERVATIONS

a	$\sin^2\theta$			a	$\sin^2\theta$		
	$x=0.3$, $k=0\ 75$	$x=0$, $k=0.71$	Observed (Blue Light)		$x=0.3$, $k=0.75$	$x=0$, $k=0.71$	Observed (Blue Light)
0.90.....	0.1145	0 1145	0 1145 (adopted)	0.98 ...	0.0586	0.0585	0.0589
.92.....	.1005	.1005	.1003	0.99 ...	.0507	.0504	.0510
.94.....	.0867	.0867	.0865	1 00..	0.0389	0.0383	0 0385
0.96.....	0 0730	0.0729	0 0732				

In a binary system for which k is near 0.75, as is true for RW Tauri, it is not possible to discriminate between various combinations of x and k in the interval $0.90 < a < 0.99$. This is seen from Table 6, which gives $\sin^2\theta$ values which were computed from the ψ tables with the adopted values of B and A. This was done for each of the limiting cases $x = 0$, $k = 0.71$, and $x = 0.3$, $k = 0.75$. The empirical values of $\sin^2\theta$ read from the smooth curve are also listed. In the region $0.2 < a < 0.8$ the two models predict values of $\sin^2\theta$ which differ little from each other. For $a < 0.2$, however, somewhat different values of $\sin^2\theta$ result. This is seen in Figure 3, where the two curves and the normal points are plotted. The model $x = 0.3$, $k = 0.75$ gives a slightly better fit but is still not very satisfactory. Any further lowering of the curve in this range of a is ruled out by the restriction that $\cot^2 i \geq 0$ (cf. eq. [5]).

In the intermediate solution, improvement in the elements may be made by one of several methods using least squares. For instance, the values of ψ, A, and B may be changed simultaneously for a best fit (Russell and Merrill 1953). However, then infinite weight is still given to two points on the light-curve. Alternately, a least-squares solution may be made with the fundamental relation

$$\sin^2\theta \sin^2 i + \cos^2 i = r_K^2 (1 + kp)^2 , \tag{6}$$

where $p = (\delta - r_K)/r_B$ and δ is the projected separation of the centers of the stars. This is the method adopted by Kopal (1950). In the third method, differential corrections are applied to the residuals in intensity from the normals in the preliminary solution. This has been discussed by Irwin (1947). All three methods take into account the weights of the individual normal points, which have two aspects—the empirical, w_e, and the intrinsic, w_i. The former depends on the error of an individual observation and the number of points in a normal. The observational errors are generally equal on a magnitude scale (as contrasted with equal errors on an intensity scale), since the sky fluctuations predominate. With fainter objects the sky background contributes a greater share to the observed signal, especially with moonlight, and the instrumental noise increases in importance. In the present study the mean error of a single observation for an 8.0-mag. star was equal to ± 0.004 mag. and for a 12.5-mag. star was ± 0.020 mag. For the intermediate magnitudes the observational error was determined as a function of magnitude from the residuals during totality in each spectral region.

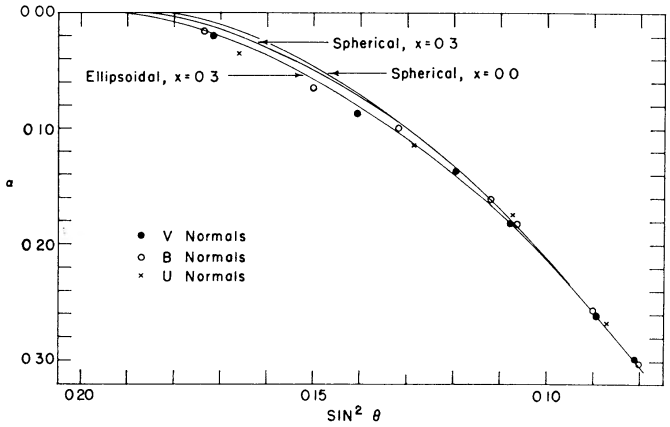

FIG. 3.—The light-curve near first contact. Normal points in the three spectral regions are plotted against $\sin^2 \theta$, which is related to the phase. Three models are shown: spherical with a limb-darkening coefficient of $x = 0.0$; the same with $x = 0.3$; and the ellipsoidal model adopted in Section V, which gives the best fit.

For the case in which errors are equal on a magnitude scale, the intrinsic weight is given (Kopal 1950) by

$$\sqrt{w_i} = \frac{1}{l} \frac{dl}{d \sin^2 \theta} . \tag{7}$$

Values of $\Delta l/\Delta \sin^2 \theta$, separate for different l, were found from the normals, and then $dl/d \sin^2 \theta$ was derived by a smoothing procedure. Because of the enormous change in luminosity during eclipse, $\sqrt{w_i}$ varies through a range of 1:180 between maximum and minimum. The square root of the total weight, $\sqrt{(w_e \times w_i)}$, varies between 1 and 39 because the empirical weights are less near minimum.

In Kopal's method the equations of condition for the least-squares solution are used in the form

$$(p^2 - 1) C_1 + 2 (p + 1) C_2 + C_3 = \sin^2 \theta . \tag{8}$$

Here $C_1 = r_K \csc^2 i; C_2 = r_B r_K \csc^2 i; C_3 = \sin^2 \theta''$, where θ'' is the phase angle at internal tangency and p was defined following equation (6). Assuming $x = 0$ and $k = 0.70$, each observed α_i leads to a value of p from Tsesevich's (1940) tables. The solution for all 30 normals in blue light with their appropriate weights give $r_B = 0.1783$, $r_K = 0.2484$, $k = 0.7180$, and $i = 88°.19$. To evaluate the effect of the first three normal

points, which were somewhat discordant, a solution was also carried out with the other 27 points only. This resulted in $r_B = 0.1760$, $r_K = 0.2487$, $k = 0.7707$, and $i = 87°.86$.

This latter solution agrees with the model derived above from the ψ tables and $x = 0$, where only the region $\alpha > 0.90$ was used. Therefore, with the adopted weights, the normals for which α is small contribute little to the solution. Irwin (1947) makes the comment: "The method of least squares is no substitute for good judgment on the part of the computer." It is the writer's opinion that adoption of the model with $x = 0.3$ and $k = 0.748$ is the more realistic. As the limb darkening appears to be less in the visual and ultraviolet regions, the light-curve could not be satisfied by the geometrical elements derived from the blue solution and $x = 0$. The present theory of limb darkening also makes a model with $x > 0$ preferable. The (O − C) residuals, computed from the blue solution with $x = 0.3$ and the U and V observed normals, are found in order to determine a correction to the limb darkening in these two spectral regions. Any systematic difference is attributed to limb darkening, as the geometrical elements may be presumed to be equal. On this basis the values $x_B - x_V = 0.10$ and $x_B - x_U = 0.06$ are found to give the best fit to the observed normals.

TABLE 7

PHOTOMETRIC MODEL OF RW TAURI

Ratio of radii	0.748
Radius of B star	0.1852
Radius of K star	0.2469
Inclination of the orbit	90.00° (adopted)
Ratio of surface brightnesses, J_K/J_B	U:0.0024 B:0.0056 V:0.0142
Limb-darkening coefficients of star B	x_U=0.24 x_B=0.30 (adopted) x_V=0.20

The final residuals are given in Table 5. They are quite satisfactory for the blue and visual observations, but the ultraviolet residuals are systematically negative for larger values of l. No change in the elements seems possible without affecting the B and V observations adversely. Possibly a more careful rectification is needed in the ultraviolet; more observations outside eclipse would be necessary to achieve this.

In all three spectral regions there remain significantly positive residuals for $\alpha < 0.2$. This is discussed in the next section, where the shape of the K star is discussed in more detail. Table 7 gives the adopted values for the final model.

V. DISCUSSION

Hiltner and Hardie's (1949) velocity-curve of RW Tauri yielded an eccentricity of 0.29. If this system is similar to U Cephei (Hardie 1950), this eccentricity is spurious, and circular elements are to be preferred. A value of 40 km/sec for the velocity semi-amplitude of RW Tauri may then be adopted. This leads to a mass function of 0.0174 $\odot$, which is quite small. The mass ratio, $\mathfrak{M}_B/\mathfrak{M}_K$, of the eclipsing pair is not available from the spectroscopic observations, as the K star is not observed except during totality. However, an upper limit to the mass ratio may be set by assuming that the K star fills the inner equipotential surface through the Lagrangian point. There is reason to believe that this situation actually exists because of the large radius of the K star and the presence of an emission ring around the B star. The limiting mass ratio arises because the dimensions of the equipotential surface are smaller for more extreme mass

ratios. With the adopted radius (in the equatorial plane perpendicular to the line joining the stars) of $r_K = 0.247$, a value of $\mu = \mathfrak{M}_B/(\mathfrak{M}_B + \mathfrak{M}_K)$ is found to be 0.177 by interpolation in Kuiper and Johnson's (1956) table. Therefore, the upper limit to the mass ratio is 4.65.

A radius of 1.5×10^6 km for the orbit of the B star around the center of gravity is found from the period and velocity semiamplitude. With the above mass ratio and $i = 90°.0$, the semimajor axis of the eclipsing system is 8.5×10^6 km. Kepler's laws may then be applied, giving $(\mathfrak{M}_B + \mathfrak{M}_K) = 3.1 \odot$. Therefore, $\mathfrak{M}_B = 2.55 \odot$ and $\mathfrak{M}_K = 0\ 55 \odot$, and the radii are $R_B = 2.25 \odot$ and $R_K = 3.0 \odot$. For the B star these are in general agreement with the mass-luminosity and mass-radius relations (Kuiper 1938), but the K star shows a definite deviation. Since the $\mathfrak{M}$–L relation gives $L_B/L_K = 470$, it might be argued that the residual light observed at totality is not due largely to the K star but mainly to stars C and D. However, by attributing to D all the light of the K star, the $\mathfrak{M}$–L situation for D is scarcely improved. Therefore, we shall adopt M_V (K) $= +3.4$, $\mathfrak{M}_K = 0.55 \odot$, and M_{bol} (K) $= +3.3$. Kuiper's $\mathfrak{M}$–L relation would give M_{bol} (K) $= 9.8$, or a departure of -6.5 mag. in luminosity. This places the star in the group of subgiants, discussed by Wood (1950), Struve (1953), and Crawford (1955), which are much larger and more luminous than the $\mathfrak{M}$–L and $\mathfrak{M}$–R relations would indicate. If the K star were plotted on Struve's Figure 3 (which shows the departure from the $\mathfrak{M}$–L relation as a function of the mass ratio for subgiant components), it would agree moderately well with other stars.

It seems likely that Crawford's model, in which the subgiant component fills the inner zero-velocity (equipotential) surface, is applicable here. In this case any slight instability will cause matter to leave the K star at the inner Lagrangian point, L_1 (Kuiper 1941, case A), and subsequently circle around the B star. This would explain not only the existence of the emission ring around the B star but also the high rotational velocity of 350 km/sec of the emission and its fluctuations in intensity (Joy 1947). This velocity is compatible with that attained by matter at L_1 falling to the surface of the B star. Joy found that the red emission component (material receding from the K star) was stronger, on the average, than the violet component. This is consistent with the above model, in that the mass leaving the K star will have undergone less dispersion and diffusion when it first starts around the B star.

There remains the problem of the relatively large positive residuals from the light-curve near first contact. If the above model is adopted in which the K star fills its inner zero-velocity surface, the spherical approximation used in the photometric solution is no longer applicable. Departure from the spherical model will not significantly affect the light-curve outside eclipse because the distorted K star contributes so little light to the system. The B star will be much less distorted because of its greater density. Ordinary rectification procedures do not apply in this case, as similar ellipsoids cannot be assumed. The observations near first contact deviate from the spherical model in the expected sense: at a given phase a larger fraction of the light of the B star is eclipsed than a spherical model would indicate. The observations near second and third contact, which determine the radius of the K star in the photometric solution, refer to the projected radius of the ellipsoid observed at that phase. This radius is less than the projected radius near first contact. If the ratio of the axes in the orbital plane as given by the equipotential surface is adopted, namely, $b/a = 0.247/0.280$, the projected radius, b', at first contact is 0.252. Although tables considering a spherical star eclipsed by an ellipsoid are not available, the limiting circular values may be used in forming an estimate. With the value of the projected radius appropriate for each phase, a new determination of $\alpha = f(\sin^2 \theta)$ is made. The agreement with the observations in the region $\alpha < 0.2$ is considerably improved (see Fig. 3); the fit near second contact is assured by the choice of $b = 0.247$. In the intermediate portion of the light-curve the radius along the third axis, c, is important. Its value is 0.237 and remains constant throughout

the eclipse, since $i = 90°$. Thus it is found that this model can account satisfactorily for the observed light-curve. It may also possibly explain the low value of the derived limb-darkening coefficient, but it would require more extensive rectification procedures to establish this. The properties of the stars are summarized in Table 8; estimates of the errors are included.

It is a pleasure to record my thanks to Dr. G. P. Kuiper for many helpful discussions. Thanks are also due to Drs. A. Blaauw and H. L. Johnson, who kindly made available their observing time and photometer on November 24, 1955. I am indebted to the National Science Foundation for a predoctoral fellowship while pursuing this work. I should like to acknowledge the assistance of my wife, Patricia, in the computations and other technical work.

TABLE 8

PHYSICAL PROPERTIES OF THE ECLIPSING COMPONENTS

Spectral type	B8 Ve	K0 IV
Mass (⊙)	2 55±0.05	0.55±0.05
Radius (⊙)	2.25±0 05	*a*: 3.40±0.10 *b*: 3.00±0.10 *c*: 2.90±0.10
Density (⊙)	0.22±0 22	0 018±0.003
M_V	−0.5 (adopted)	+3.4±0.1

REFERENCES

Binnendijk, L. 1941, *B.A.N.*, **9**, 173.
Crawford, J. A. 1955, *Ap. J.*, **121**, 71.
Dugan, R. S., and Wright, F. H. 1938, *Princeton Contr.*, **19**, 28.
Hardie, R. H. 1950, *Ap. J.*, **112**, 542.
Hertzsprung, E. 1928, *B.A.N.*, **4**, 179.
Hiltner, W. A., and Hardie, R. H. 1949, *Ap. J.*, **110**, 438.
Hiltner, W. A., and Johnson, H. L. 1956, *Ap. J.*, **124**, 367.
Irwin, J. B. 1947, *Ap. J.*, **106**, 380.
Johnson, H. L., and Harris, D. L. 1954, *Ap. J.*, **120**, 196.
Johnson, H. L., and Morgan, W. W. 1951, *Ap. J.*, **114**, 522.
———. 1953, *ibid.*, **117**, 313.
Joy, A. H. 1942, *Pub. A.S.P.*, **54**, 35.
———. 1947, *ibid.*, **59**, 172.
Keenan, P. C., and Morgan, W. W. 1951, *Astrophysics*, ed. J. A. Hynek (New York: McGraw-Hill Book Co.), p. 12.
Kopal, Z. 1950, *Harvard Mono.*, No. 8.
Kuiper, G. P. 1938, *Ap. J.*, **88**, 472.
———. 1941, *ibid.*, **93**, 133.
Kuiper, G. P., and Johnson, J. R. 1956, *Ap. J.*, **123**, 90.
Merrill, J. E. 1950, *Princeton Contr.*, Vol. **23**.
Russell, H. N., and Merrill, J. E. 1953, *Princeton Contr.*, Vol. **26**.
Sharpless, S. 1952, *Ap. J.*, **116**, 251.
Struve, O. 1953, *Mém. Soc. R. Liège*, **14**, 236.
Tsesevich, V. T. 1940, *Astr. Inst. Leningrad*, Vol. **3**, No. 50.
Wood, F. B. 1950, *Ap. J.*, **112**, 196.
Wright, F. W. 1934, *Harvard Ann.*, **89**, 171.
Wyse, A. B. 1934, *Lick Obs. Bull.*, **17**, 42.